NIH Public Access
Author Manuscript
Acad Radiol. Author manuscript; available in PMC 2014 September 01.

Published in final edited form as:
Acad Radiol. 2013 September ; 20(9): . doi:10.1016/j.acra.2013.04.013.

Noninvasive phosphorus magnetic resonance spectroscopic imaging predicts outcome to first-line chemotherapy in newly diagnosed patients with diffuse large B-cell lymphoma

Fernando Arias-Mendoza, MD, PhD[1], **Geoffrey S. Payne, PhD**[2], **Kristen Zakian, PhD**[3], **Marion Stubbs, PhD**[4,†], **Owen A. O'Connor, MD, PhD**[5], **Hamed Mojahed, PhD**[1], **Mitchell R. Smith, MD**[6], **Adam J. Schwarz, PhD**[2], **Amita Shukla-Dave, PhD**[3], **Franklyn Howe, PhD**[7], **Harish Poptani, PhD**[8], **Seung-Cheol Lee, PhD**[8], **Ruth Pettengel, MD**[9], **Steven J. Schuster, MD**[10], **David Cunningham, MD**[11], **Arend Heerschap, PhD**[12], **Jerry D. Glickson, PhD**[8], **John R. Griffiths, PhD**[4], **Jason A. Koutcher, MD, PhD**[3], **Martin O. Leach, PhD**[2], and **Truman R. Brown, PhD**[1]

[1]Department of Radiology, Columbia University, New York City, New York, USA [2]Department of Radiology, Royal Marsden Hospital & Institute of Cancer Research, London, United Kingdom [3]Department of Radiology, Memorial Sloan Kettering Cancer Center, New York City, New York, USA [4]Department of Radiology, CR UK Cambridge Research Institute, Cambridge, United Kingdom [5]Department of Medicine and Oncology, Columbia University Medical Center, New York City, New York, USA [6]Department of Medical Oncology, Fox Chase Cancer Center, Philadelphia, Pennsylvania, USA [7]Department of Radiology, St. George's Hospital, London, United Kingdom [8]Department of Radiology, The University of Pennsylvania, Philadelphia, Pennsylvania, USA [9]Department of Medical Oncology, St. George's Hospital, London, United Kingdom [10]Abramson Cancer Center, Perelman Center for Advanced Medicine, The University of Pennsylvania, Philadelphia, Pennsylvania, USA [11]Section of GI and Lymphoma Units, Department of Medicine, Royal Marsden Hospital & Institute of Cancer Research, London, United Kingdom [12]Department of Radiology, Radboud University Nijmegen Medical Centre, Nijmegen, The Netherlands

Abstract

Rationale and Objectives—Based on their association with malignant proliferation, using noninvasive phosphorus MR spectroscopic imaging (^{31}P MRSI), we measured the tumor content of the phospholipid-related phosphomonoesters (PME), phosphoethanolamine and phosphocholine and its correlation with treatment outcome in newly diagnosed diffuse large B-cell lymphoma (DLBCL) patients receiving standard first-line chemotherapy.

Experimental Design—The PME value normalized to nucleoside triphosphates (PME/NTP) was measured using ^{31}P MRSI in tumor masses of 20 DLBCL patients prior to receive standard

© 2013 The Association of University Radiologists. Published by Elsevier Inc. All rights reserved

Corresponding author: Dr. Fernando Arias-Mendoza, Associate Professor of Clinical Radiology (Physics), Department of Radiology, Columbia University Medical Center, 710 W 168th St., Neurological Institute Basement, Room B-057, New York, NY 10032, USA, Telephone: 1-212-305-1169, Facsimile: 1-212-342-5773, fa2003@columbia.edu.
†Deceased and to whom this paper is dedicated

Publisher's Disclaimer: This is a PDF file of an unedited manuscript that has been accepted for publication. As a service to our customers we are providing this early version of the manuscript. The manuscript will undergo copyediting, typesetting, and review of the resulting proof before it is published in its final citable form. Please note that during the production process errors may be discovered which could affect the content, and all legal disclaimers that apply to the journal pertain.

Conflict of Interest Disclosure:
The authors have declared no conflict of interest.

NIH-PA Author Manuscript
NIH-PA Author Manuscript
NIH-PA Author Manuscript

NIH-PA Author Manuscript

NIH-PA Author Manuscript

NIH-PA Author Manuscript

first-line chemotherapy. Response at six months was complete in 13 patients and partial in seven. Time to treatment failure (TTF) was ≤11 months in eight patients, from 18 to 30 months in three, and ≥ 60 months in nine.

Results—On a t-test, the pretreatment tumor PME/NTP mean value (SD, n) of patients with a complete response at six months was 1.42 (0.41, 13), which was significantly different from the value of 2.46 (0.40, 7) in patients with partial response ($p < 0.00001$). A Fisher test significantly correlated the PME/NTP values with response at six months (sensitivity and specificity at 0.85, $p < 0.004$) while a Cox proportional hazards regression significantly correlated the PME/NTP values with TTF (hazard ratio=5.21, $p < 0.02$). A Kaplan-Meier test set apart a group entirely composed of patients with TTF ≤ 11 months (hazard ratio=8.66, $p<0.00001$).

Conclusion—The pretreatment tumor PME/NTP values correlated with response to treatment at six months and time to treatment failure in newly diagnosed DLBCL patients treated with first-line chemotherapy and therefore they could be used to predict treatment outcome in these patients.

Keywords

In vivo; lymphoma; metabolic imaging; MR spectroscopy; prediction of therapy outcome

Introduction

For many cancer patients established first-line therapies are either ineffective or initially effective but not curative. For instance, 63% of patients with diffuse large B-cell lymphoma (DLBCL) show a complete response to first-line therapy, but only 40% have prolonged survival (1, 2). An *a priori* method to identify unresponsive patients to standard treatments would be of extreme value to offer these patients alternate treatment options, thereby maximizing therapeutic success, sparing toxicity, and lowering healthcare costs.

Newly diagnosed DLBCL patients receive equivalent first-line chemotherapy regardless of the substandard treatment outcome on a large number of patients. Over the years, the most common regimen has been CHOP, a doxorubicin-based drug cocktail with added cyclophosphamide, vincristine, and prednisone (2). Other first-line multi-drug treatments can be used to treat DLBCL but their mechanisms of action and response rates are similar to CHOP, therefore they are considered comparable (CHOP-like therapy). Only recently rituximab has been added to first-line regimens to treat DLBCL (i.e., R-CHOP) increasing relapse-free and overall survival (3, 4). However, even though rituximab has improved treatment outcome, still a significant proportion of patients experience early treatment failure, partial response, or recurrence. A method that could appropriately and timely identify high-risk newly diagnosed DLBCL patients bound to be unresponsive to the established first-line therapies should allow early consideration of alternate treatments, like high-dose therapy, autologous stem cell transplantation (5), and/or promising new agents that target cellular signaling processes (6–9), with the aim to maximize therapeutic success in high-risk patients without compromising those patients who will respond to the present standard of care.

Metabolic profiles, especially those measured using molecular imaging could be of value to risk-stratify cancer patients. The tumor uptake of ^{19}F-fluorodeoxyglucose (FDG) visible by positron emission tomography (PET)(10–13) and our recent studies following phospholipid-related biomarkers using ^{31}P magnetic resonance spectroscopic imaging (^{31}P MRSI)(14–16) are two examples of these metabolic profiles. FDG-PET is extensively used for prognosis, early response assessment, and post-treatment response assessment in DLBCL based on the comparisons of interim and late-treatment FDG-PET scans with pretreatment scans (17–19). Alternatively, our preliminary results have suggested a correlation between the pretreatment

NIH-PA Author Manuscript

NIH-PA Author Manuscript

NIH-PA Author Manuscript

phospholipid-related profiles measured noninvasively by ^{31}P MRSI and response to therapy in lymphomas (14).

We aimed to demonstrate if ^{31}P MRSI can obtain reproducible intra-tumor information in realtime (before treatment is instituted) to predict chemotherapeutic response. This aim was based on 1) the relatively large quantities of the phospholipid-related phosphomonoesters (PME) phosphoethanolamine and phosphocholine reported in tumors of diverse origin using ^{31}P MRSI (20, 21); 2) the reported increase of the tumor content of PME during rapid tumor proliferation and invasive growth and decrease during remission and responsiveness to chemotherapy (20, 22); and 3) our preliminary results linking the intracellular PME value with treatment outcome in lymphoma patients (14).

To fulfill this aim we analyzed newly diagnosed DLBCL patients that underwent standard first-line therapy in the form of CHOP or equivalent chemotherapy (CHOP-like therapy) following the REMARK guidelines (23). In these patients we assessed if the PME tumor value measured prior to initiating treatment could predict two objective parameters of outcome of therapy, response at six months and time to treatment failure (TTF). Our data confirmed that the pretreatment PME tumor value, when normalized to the tumor content of nucleoside triphosphates (PME/NTP) correlated with both parameters of outcome and discriminated a group of DLBCL patients who had an early failure to CHOP-like therapy (≤ 11 months). The significance of this work is the potential use of the noninvasive molecular imaging measurement of the pretreatment tumor PME/NTP value as a prediction biomarker of therapy outcome in DLBCL patients, and probably in other aggressive forms of cancer.

Patients and Methods

Patients

The protocol to study lymphoma patients noninvasively using ^{31}P MRSI by our cooperative consortium was approved at each institution by the corresponding Institutional Review Board (US) or Ethical Committee (EU). Signed consent for the study from each subject was obtained after the nature of the procedure was fully explained, and the coordinating institution maintained a cooperative Institutional Review Board approval to enforce all regulations set by the sponsor (the National Cancer Institute of the National Institutes of Health, US). Patients for the present study were selected from a large database of diverse lymphoma patients (more than 250 patients) who received treatment and follow-up at our institutions and which were accrued aided by the treating physicians. These patients were studied prospectively aiming to assess if tumor information acquired using ^{31}P MRSI noninvasively could derive in parameters that could predict or prognosticate response to treatment. Eligibility criteria for the present analysis were patients with histologically confirmed, previously untreated DLBCL tumors that received first-line doxorubicin-based multidrug chemotherapy or equivalent (CHOP-like therapy), who had a ^{31}P MRS exam from a target tumor region within the 15 days before treatment, and had at least the minimum quality requirements for the ^{31}P tumor spectrum described below. Patients treated with added rituximab were excluded from the present analysis.

Study design

The content of the phospholipid-related phosphomonoesters (PME), phosphoethanolamine and phosphocholine was determined within the 15 days prior to the start of CHOP-like chemotherapy in the *in vivo* ^{31}P MR spectrum of tumor masses of newly diagnosed DLBCL patients. The content of nucleoside triphosphates (NTP) measured in the same *in vivo* ^{31}P MR tumor spectra was used to normalize the PME value (PME/NTP) to allow adequate inter-patient and inter-institutional comparisons (15). Quality criteria for the study were a

NIH-PA Author Manuscript

NIH-PA Author Manuscript

NIH-PA Author Manuscript

signal to noise ratio for the Pβ resonance of NTP of at least 2.0 and minimal contamination from adjacent tissues.

The pretreatment tumor PME/NTP value was tested for its correlation with response to chemotherapy at six months and time-to-treatment failure (TTF). Response to treatment was assessed by volumetric changes of enlarged lymph nodes using standard categorization (24). TTF was defined as the time in months from the start of the first-line treatment to the onset of the subsequent treatment (25). The clinical features to determine IPI were assessed at the time of diagnosis as originally reported (26).

Assay method

We have developed a highly standardized noninvasive ^{31}P MRSI determination to study tumor masses in readily available clinical MR systems (14, 21). With this methodology we can obtain comparative results when the tumor content of nucleosides triphosphates (NTP), a surrogate measure of cellular viability (15), is used to normalize the PME value (PME/NTP) (14).

Each patient had a noninvasive ^{31}P MRSI exam from a target tumor mass selected based on superficiality and size (≥30 millimeters in each dimension). The exam was acquired within the 15 days before treatment (17 patients within the four-day period prior, one patient 10 days before, and two 15 days before treatment started). The ^{31}P MRSI exam was acquired using 1.5 Tesla clinical MR systems as described elsewhere (14). In brief, MR images were acquired followed by optimization of the homogeneity of the local magnetic field and the acquisition of 3D-localized ^{1}H-decoupled chemical shift imaging of ^{31}P signals with the following conditions: eight phase-encoding steps and 240 millimeters of field of view in each dimension, a 45° flip angle at the location of the tumor, 512 data points, spectral width of ± 1000 Hertz, repetition time of one second, constant amplitude phase-modulated ^{1}H decoupling during the acquisition time, low-level ^{1}H excitation during the rest of the time for nuclear Overhauser effect, and four averages per encoding step.

The acquired ^{31}P spectral data sets were Fourier transformed in the spatial domain and in the time domain were zero-filled to 1024 points, filtered with a Lorentzian function of 5–7Hz, Fourier transformed, and phase corrected. Using the MR images, the data sets were voxel-shifted to locate at least one voxel entirely inside the tumor mass and minimizing spectral contamination from surrounding tissues. If more than one clean tumor-containing voxel was obtained, the spectra were averaged to produce a single tumor spectrum per patient, where the signals of phosphomonoesters (PME), and the Pβ signal of nucleoside triphosphates (NTP) were integrated and the pretreatment tumor PME/NTP ratio calculated (Figure 1).

Statistical Analyses

The ability of the pretreatment PME/NTP and IPI values to correlate and thus predict response to therapy at six months was assessed using two-tailed, two-sample Student's t-tests, receiver operator characteristic (ROC) curves, and Fisher probability tests. Two-tailed F tests showed that the parameters in all the test groups had equal variances, thus t-tests were performed accordingly. For comparisons, Fisher probability tests were performed creating contingency tables using as cutoff the maximum of the Youden index in the ROC tests (J = max [sensitivity$_i$ + specificity$_i$ −1]). The statistical significance of the pretreatment PME/NTP and IPI values to predict time to treatment failure (TTF) was assessed using the Cox proportional hazards survival regression and Kaplan-Meier survival curves. *Post-hoc*, two-tailed power analyses were performed to determine statistical effect size and statistical power considering both adequate at ≥ 0.8 (27). All the statistical analyses except the power calculations were performed using the IBM SPSS Statistics software package (SPSS, Inc.,

NIH-PA Author Manuscript

NIH-PA Author Manuscript

NIH-PA Author Manuscript

IBM Company Headquarters, Chicago IL, USA). The G*Power analysis package release 3 was used for the power calculations (28).

Results

Patient population

Table 1 summarizes the characteristics of the study population. The median age of the population was 59 years (range 19–85) and 45% (n=9) of the patients were female. The 20 patients included in the study received CHOP-like therapy. Fourteen received doxorubicin-based therapy in the form of CHOP alone (12 patients, acronyms for the drug cocktails are defined in the footnotes of Table 1), CHOP with ICE (one patient), and ProMACE-CytaBOM (one patient). Two patients received mitoxantrone-based therapy in the form of CNOP and PMitCEBO, respectively. The medical charts of the remaining four patients did not clearly specify the treatment received. However, the charts stated that the patients received CHOP-like treatment, allowing their inclusion in this study. Treatments were at the discretion of the treating clinician reflecting the established standard of care at each international institution. This apparent treatment variability could be misinterpreted as being against the REMARK guidelines for proper testing of biomarkers of response (23), but it has been extensively demonstrated that treatments listed in table I are equivalent (29, 30) because they exert a similar mechanism of action at the cellular level (i.e., type II DNA topoisomerase inhibition and DNA intercalation) and have similar risk for survival.

Based on IPI, the cohort was stratified in eight patients with low-risk (two patients with IPI 0 and six with IPI 1), six with low-intermediate risk (IPI 2), four with high-intermediate risk (IPI 3), and two with high risk (both with IPI 4; no patients with IPI 5). The response to treatment at six months divided the patients in 13 with complete response, seven with partial response, and none with stable or progressive disease. During the observation period, 11 patients failed treatment, five reached the end of the observation period without failing, and four were lost to the study (two were lost to follow up and two died of unrelated causes). The last nine patients were assigned as censored cases. The follow up time was ≤11 months in eight patients (two censored), from 18 to 30 months in three (two censored), and ≥60 months in nine (five censored).

Descriptive statistics

The correlation of the pretreatment PME/NTP and IPI values are summarized in Tables 2 and 3. In t-tests (Table 2), the pretreatment tumor PME/NTP mean value of the patients that exhibited complete response was statistically lower in comparison to those patients that exhibit incomplete response ($p < 0.00001$). In comparison, the IPI mean value distinguished two groups with poor significance ($p < 0.06$) for the same response groups. Using the maximum of the Youden index of the ROC curves as cutoff for comparable Fisher tests (Table 2), the pretreatment PME/NTP values showed significance to correlate with response at six months (cutoff at 1.92, sensitivity=0.85, specificity=0.86, $p < 0.01$) while the IPI values did not show significance. In addition, because it is clinically important to maximize the correct assignment of patients that will respond to therapy, instead of using the maximum of the Youden index, the PME/NTP cutoff was moved to maximize sensitivity in a Fisher test. The sensitivity and specificity using this cutoff (2.2) was 1.0 and 0.71, respectively.

Survival tests

The PME/NTP values significantly correlated with TTF with a hazard ratio of 5.21 ($p<0.02$) in Cox proportional hazards survival regression. The Kaplan-Meier survival test showed that the PME/NTP values set apart two patient groups with significantly different TTF curves

NIH-PA Author Manuscript

NIH-PA Author Manuscript

NIH-PA Author Manuscript

when the cutoff was set at 2.2 ($p<0.00001$). The hazard ratio between the two curves in the Kaplan-Meier survival test was 8.66. In comparison, the IPI correlation with TTF was not significant in both the Cox proportional hazards survival regression (hazard ratio of 1.73, $p<0.06$) and the Kaplan-Meier test ($p<0.14$).

Power Calculations

The strong significance of the correlation between the tumor PME/NTP values and these measures of treatment outcome despite our modest sample size attests of a large statistical effect size for our biomarker. This was corroborated by *post hoc* power calculations (27, 28), where the calculated statistical effect size for the t-, Fisher, and Kaplan-Meier tests was always large (>1.2) and the statistical power was always highest (1.00). However, the analysis of this cohort failed to show correlation between IPI and treatment outcome. This lack of correlation is mostly due to the reported small statistical effect size of the IPI as predictor of outcome (31).

Discussion

Our results confirmed in a standardized patient cohort (i.e., newly diagnosed previously untreated DLBCL patients under CHOP-like chemotherapy) that the pretreatment tumor PME/NTP values correlate with response to treatment at six months and time to treatment failure (TTF) (23). Importantly, our results show that the low survival risk group generated by the Kaplan-Meier survival analysis (Figure 2), was composed of five of the eight patients with TTF ≤11 months plus none of these patients were censored. From the remaining three patients with TTF ≤11 months, two were censored due to reasons unrelated to the disease. Thus, five of the six patients (83%) that in fact reached TTF at ≤11 months (not censored) were classified in the low survival risk group whereas no patients with TTF >11 months were included in this group.

We consider that the strong effect size of the correlation between the pretreatment tumor PME/NTP value and the two parameters of therapy outcome (response at six months and TTF) is because the PME/NTP value directly assesses the extent of disruption of the phospholipid metabolism, important metabolic process associated with a variety of cellular control mechanisms in proliferating tissues, (14, 15, 20–22). An important growth control mechanism in phospholipid metabolism is when phospholipids are hydrolyzed by phospholipase C into the corresponding PME and diacylglycerol, the latter implicated in cell cycle signaling and apoptosis (32, 33). Demonstration of the effects of the genetic dysregulation of phospholipase C in tumor progression has been reported (34). A growing body of evidence also points to the role of phospholipase C in processes crucial to cell signaling, activation of cells of the immune system, and programmed cell death (35, 36). The increase of the phosphomonoesters (PME) phosphoethanolamine and phosphocholine during rapid tumor proliferation and invasive growth and their marked reduction during remission and responsiveness to cancer therapy (14, 20) could be related to modifications on the activity of this hydrolytic enzyme. This evidence strongly suggests a correlation between the PME tumor concentration with tumor growth, invasive potential, and/or reduction of apoptotic capability (14, 20, 35–38), which in turn are processes clearly associated with poorer clinical outcomes (32–34).

Since the determination of the tumor PME/NTP value by ^{31}P MRSI is noninvasive, obtained prior to the start of therapy, and has high statistical power, it makes it potentially useful to risk-stratify patients prior to receive treatment. However, the low sensitivity of ^{31}P MRSI and concomitant need for long acquisition times and low spatial resolution need to be addressed before it can be used as a standard tool on the clinic. Nevertheless, the real-time predictive information of the pretreatment tumor value of PME/NTP could complement

NIH-PA Author Manuscript

NIH-PA Author Manuscript

NIH-PA Author Manuscript

other methodologies that also determine predictive or prognostic biomarkers of response like FDG-PET (17–19), gene expression profiling (39, 40), and immunohistochemistry (41–43). For example, the fact that PME/NTP and FDG-PET evaluate different tumor metabolic pathways (phospholipid turnover and anaerobic glycolysis, respectively) could make the determination of PME/NTP by ^{31}P MRSI and FDG by PET complementary for the assessment of treatment response in DLBCL.

In summary, we have successfully demonstrated that the pretreatment tumor PME/NTP value determined noninvasively by ^{31}P MRS provides important information towards predicting response to treatment for newly diagnosed DLBCL patients receiving CHOP-like therapy. Though in their infancy, it is clear that this and other metabolic imaging approaches can offer new methods for risk stratification and determination of early response to cancer treatments, complementing and extending established models and facilitating the design of personalized therapy.

Acknowledgments

Additional participants who contributed in the present research program were Ahmed Sawas (Columbia University Medical Center), Jaime Cruz-Lobo (Columbia University Medical Center), and Mary McLean (CR UK Cambridge Research Institute).

This work was supported by National Institute of Health (US) grants 5R01CA118559 (TRB/FAM) and 5R21CA152858 (FAM). Support has also been received for the CRUK and EPSRC Cancer Imaging Centre in association with the MRC and the Department of Health (UK) under grant C1060/A10334, and NHS funding (UK) to the NIHR Biomedical Research Centre (MOL).

References

1. DeVita, V.; Hellman, S.; Rosneber, S. Cancer: principles and practice of oncology. 7th ed. Philadelphia, PA: Lippincott, Williams and Wilkins; 2001.
2. Rosen, ST.; Molina, A.; Winter, JN.; Gordon, LI.; Nicolaou, N. Non-Hodgkin's Lymphoma. In: Pazdur, R.; Hoskins, WJ.; Wagman, LD., editors. Cancer Management: A Multidisciplinary Approach. 7th ed. New York: The Oncology Group; 2003. p. 665-712.
3. Coiffier B, Lepage E, Briere J, et al. CHOP chemotherapy plus rituximab compared with CHOP alone in elderly patients with diffuse large-B-cell lymphoma. N Engl J Med. 2002; 346(4):235–242. [PubMed: 11807147]
4. Coiffier B. Rituximab and CHOP-like chemotherapy in good-prognosis diffuse large-B-cell lymphoma. Nat Clin Pract Oncol. 2006; 3(11):594–595. [PubMed: 17080173]
5. Philip T, Guglielmi C, Hagenbeek A, et al. Autologous bone marrow transplantation as compared with salvage chemotherapy in relapses of chemotherapy-sensitive non-Hodgkin's lymphoma. N Engl J Med. 1995; 333(23):1540–1545. [PubMed: 7477169]
6. O'Connor OA, Pro B, Pinter-Brown L, et al. Pralatrexate in patients with relapsed or refractory peripheral T-cell lymphoma: results from the pivotal PROPEL study. Journal of clinical oncology. 2011; 29(9):1182–1189. [PubMed: 21245435]
7. Zain JM, O'Connor O. Targeted treatment and new agents in peripheral T-cell lymphoma. International journal of hematology. 2010; 92(1):33–44. [PubMed: 20535594]
8. Wilson WH, Hernandez-Ilizaliturri FJ, Dunleavy K, Little RF, O'Connor OA. Novel disease targets and management approaches for diffuse large B-cell lymphoma. Leuk Lymphoma. 2010; 51(Suppl 1):1–10. [PubMed: 20658952]
9. O'Connor OA. Novel agents in development for peripheral T-cell lymphoma. Semin Hematol. 2010; 47(Suppl 1):S11–S14. [PubMed: 20359580]
10. Sasaki M, Kuwabara Y, Koga H, et al. Clinical impact of whole body FDG-PET on the staging and therapeutic decision making for malignant lymphoma. Annals of nuclear medicine. 2002; 16(5): 337–345. [PubMed: 12230093]

NIH-PA Author Manuscript

NIH-PA Author Manuscript

NIH-PA Author Manuscript

11. Hoskin PJ. PET in lymphoma: what are the oncologist's needs? Eur J Nucl Med Mol Imaging. 2003; 30(Suppl 1):S37–S41. [PubMed: 12677306]
12. Kasamon YL, Wahl RL, Swinnen LJ. FDG PET and high-dose therapy for aggressive lymphomas: toward a risk-adapted strategy. Curr Opin Oncol. 2004; 16(2):100–105. [PubMed: 15075899]
13. Kostakoglu L, Leonard JP, Coleman M, Goldsmith SJ. The role of FDG-PET imaging in the management of lymphoma. Clin Adv Hematol Oncol. 2004; 2(2):115–121. [PubMed: 16163171]
14. Arias-Mendoza F, Smith MR, Brown TR. Predicting treatment response in non-Hodgkin's lymphoma from the pretreatment tumor content of phosphoethanolamine plus phosphocholine. Acad Radiol. 2004; 11(4):368–376. [PubMed: 15109009]
15. Franks S, Smith M, Arias-Mendoza F, et al. Phosphomonoester concentrations differ between chronic lymphocytic leukemia cells and normal human lymphocytes. Leuk Res. 2002; 26(10):919. [PubMed: 12163053]
16. Lee S-C, Arias-Mendoza F, Poptani H, et al. Prediction and early detection of respone by NMR spectroscopy and imaging. PET Clin. 2012; 7:119–126. [PubMed: 22737093]
17. Moskowitz CH. Interim PET-CT in the management of diffuse large B-cell lymphoma. Hematology Am Soc Hematol Educ Program. 2012; 2012:397–401. [PubMed: 23233610]
18. Moskowitz CH, Zelenetz A, Schoder H. An update on the role of interim restaging FDG-PET in patients with diffuse large B-cell lymphoma and Hodgkin lymphoma. Journal of the National Comprehensive Cancer Network : JNCCN. 2010; 8(3):347–352. [PubMed: 20202464]
19. Moskowitz CH, Schoder H, Teruya-Feldstein J, et al. Risk-adapted dose-dense immunochemotherapy determined by interim FDG-PET in Advanced-stage diffuse large B-Cell lymphoma. J Clin Oncol. 2010; 28(11):1896–1903. [PubMed: 20212248]
20. Podo F. Tumour phospholipid metabolism. NMR Biomed. 1999; 12(7):413–439. [PubMed: 10654290]
21. Arias-Mendoza F, Payne GS, Zakian KL, et al. In vivo ^{31}P MR spectral patterns and reproducibility in cancer patients studied in a multi-institutional trial. NMR Biomed. 2006; 19(4): 504–512. [PubMed: 16763965]
22. Ronen SM, Jackson LE, Beloueche M, Leach MO. Magnetic resonance detects changes in phosphocholine associated with Ras activation and inhibition in NIH 3T3 cells. Br J Cancer. 2001; 84(5):691–696. [PubMed: 11237392]
23. McShane LM, Altman DG, Sauerbrei W, Taube SE, Gion M, Clark GM. Reporting recommendations for tumor marker prognostic studies (REMARK). J Natl Cancer Inst. 2005; 97(16):1180–1184. [PubMed: 16106022]
24. Cheson BD, Horning SJ, Coiffier B, et al. Report of an international workshop to standardize response criteria for non-Hodgkin's lymphomas. NCI Sponsored International Working Group. J Clin Oncol. 1999; 17(4):1244. [PubMed: 10561185]
25. Anonymous. [Accessed 2008] Dictionary of Cancer Terms in, http://www.cancer.gov/dictionary/.
26. Anonymous. A predictive model for aggressive non-Hodgkin's lymphoma The International Non-Hodgkin's Lymphoma Prognostic Factors Project. N Engl J Med. 1993; 329(14):987–994. [PubMed: 8141877]
27. Cohen, J. Statistical power analysis for the behavioral sciences. Second ed. Mahwah, NJ: Lawrence Erlbaum Associates; 1988.
28. Faul F, Erdfelder E, Buchner A, Lang AG. Statistical power analyses using G*Power 3.1: tests for correlation and regression analyses. Behav Res Methods. 2009; 41(4):1149–1160. [PubMed: 19897823]
29. Fisher RI, Miller TP, O'Connor OA. Diffuse aggressive lymphoma. Hematology Am Soc Hematol Educ Program. 2004:221–236. [PubMed: 15561685]
30. Miller TP, Jones SE. Chemotherapy of localised histiocytic lymphoma. Lancet. 1979; 1(8112): 358–360. [PubMed: 85006]
31. Ziepert M, Hasenclever D, Kuhnt E, et al. Standard International prognostic index remains a valid predictor of outcome for patients with aggressive CD20+ B-cell lymphoma in the rituximab era. J Clin Oncol. 2010; 28(14):2373–2380. [PubMed: 20385988]

NIH-PA Author Manuscript

NIH-PA Author Manuscript

NIH-PA Author Manuscript

32. Agarwal ML, Larkin HE, Zaidi SI, Mukhtar H, Oleinick NL. Phospholipase activation triggers apoptosis in photosensitized mouse lymphoma cells. Cancer Res. 1993; 53(24):5897–5902. [PubMed: 8261400]
33. Ferguson JE, Hanley MR. The role of phospholipases and phospholipid-derived signals in cell activation. Curr Opin Cell Biol. 1991; 3(2):206–212. [PubMed: 1652988]
34. Bertagnolo V, Benedusi M, Brugnoli F, et al. Phospholipase C-beta 2 promotes mitosis and migration of human breast cancer-derived cells. Carcinogenesis. 2007; 28(8):1638–1645. [PubMed: 17429106]
35. Ramoni C, Spadaro F, Barletta B, Dupuis ML, Podo F. Phosphatidylcholine-specific phospholipase C in mitogen-stimulated fibroblasts. Experimental cell research. 2004; 299(2):370–382. [PubMed: 15350536]
36. Spadaro F, Ramoni C, Mezzanzanica D, et al. Phosphatidylcholine-specific phospholipase C activation in epithelial ovarian cancer cells. Cancer Res. 2008; 68(16):6541–6549. [PubMed: 18701477]
37. Iorio E, Ricci A, Bagnoli M, et al. Activation of phosphatidylcholine cycle enzymes in human epithelial ovarian cancer cells. Cancer research. 2010; 70(5):2126–2135. [PubMed: 20179205]
38. Paris L, Cecchetti S, Spadaro F, et al. Inhibition of phosphatidylcholine-specific phospholipase C downregulates HER2 overexpression on plasma membrane of breast cancer cells. Breast Cancer Res. 2010; 12(3):R27. [PubMed: 20462431]
39. Alizadeh AA, Eisen MB, Davis RE, et al. Distinct types of diffuse large B-cell lymphoma identified by gene expression profiling. Nature. 2000; 403(6769):503–511. [PubMed: 10676951]
40. Rosenwald A, Wright G, Chan WC, et al. The use of molecular profiling to predict survival after chemotherapy for diffuse large-B-cell lymphoma. N Engl J Med. 2002; 346(25):1937–1947. [PubMed: 12075054]
41. Zinzani PL, Broccoli A, Stefoni V, et al. Immunophenotype and intermediate-high international prognostic index score are prognostic factors for therapy in diffuse large B-cell lymphoma patients. Cancer. 2010; 116(24):5667–5675. [PubMed: 20737566]
42. Nasr MR, Rosenthal N, Syrbu S. Expression profiling of transcription factors in B- or T-acute lymphoblastic leukemia/lymphoma and burkitt lymphoma: usefulness of PAX5 immunostaining as pan-Pre-B-cell marker. Am J Clin Pathol. 133(1):41–48. [PubMed: 20023257]
43. Choi WW, Weisenburger DD, Greiner TC, et al. A new immunostain algorithm classifies diffuse large B-cell lymphoma into molecular subtypes with high accuracy. Clin Cancer Res. 2009; 15(17):5494–5502. [PubMed: 19706817]

NIH-PA Author Manuscript

NIH-PA Author Manuscript

NIH-PA Author Manuscript

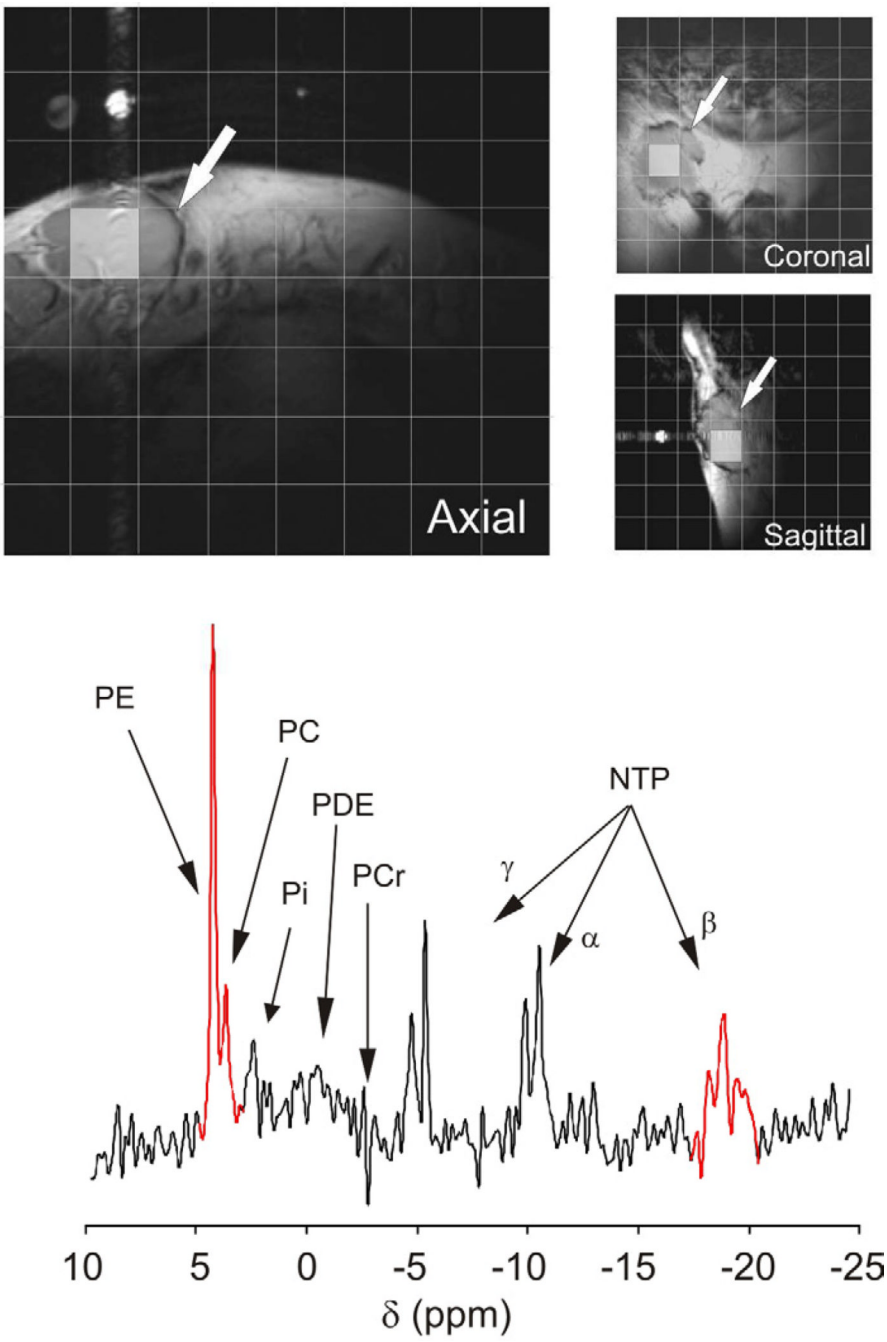

Figure 1. Example of the noninvasive 3D-localized ^{31}P MRS exam from a target tumor mass of a DLBCL patient

Top, T_1-weighted Spin-Echo MR images acquired in the three orthogonal orientations from the right inguinal area of a newly diagnosed DLBCL patient are shown. In the images a tumor mass of approximately 32–35 millimeters in each diameter is shown (white arrows). Each image is overlaid with a grid representing the projection of the 3-dimensional acquisition matrix of voxels where ^{31}P spectral signals were localized. Shaded in grey are the 2D projections of a voxel that was included in the tumor mass. **Bottom**, The ^{31}P spectrum of the voxel highlighted in the images is shown with corresponding peak assignments (PE, phosphoethanolamine; PC, phosphocreatine; Pi, inorganic phosphate;

NIH-PA Author Manuscript

NIH-PA Author Manuscript

NIH-PA Author Manuscript

PDE, the phosphodiester region; PCr, location of the phosphocreatine signal [not present in the tumor spectrum but prominent in the spectra of surrounding muscle; and NTP, the α, β, and γ phosphates of nucleoside triphosphates). The sum of the phosphomonoester (PME) signals phosphoethanolamine (PE) and phosphocholine (PC) and the triplet of the Pβ of NTP (highlighted in red in the spectrum) were integrated to obtain the tumor PME/NTP value.

NIH-PA Author Manuscript

NIH-PA Author Manuscript

NIH-PA Author Manuscript

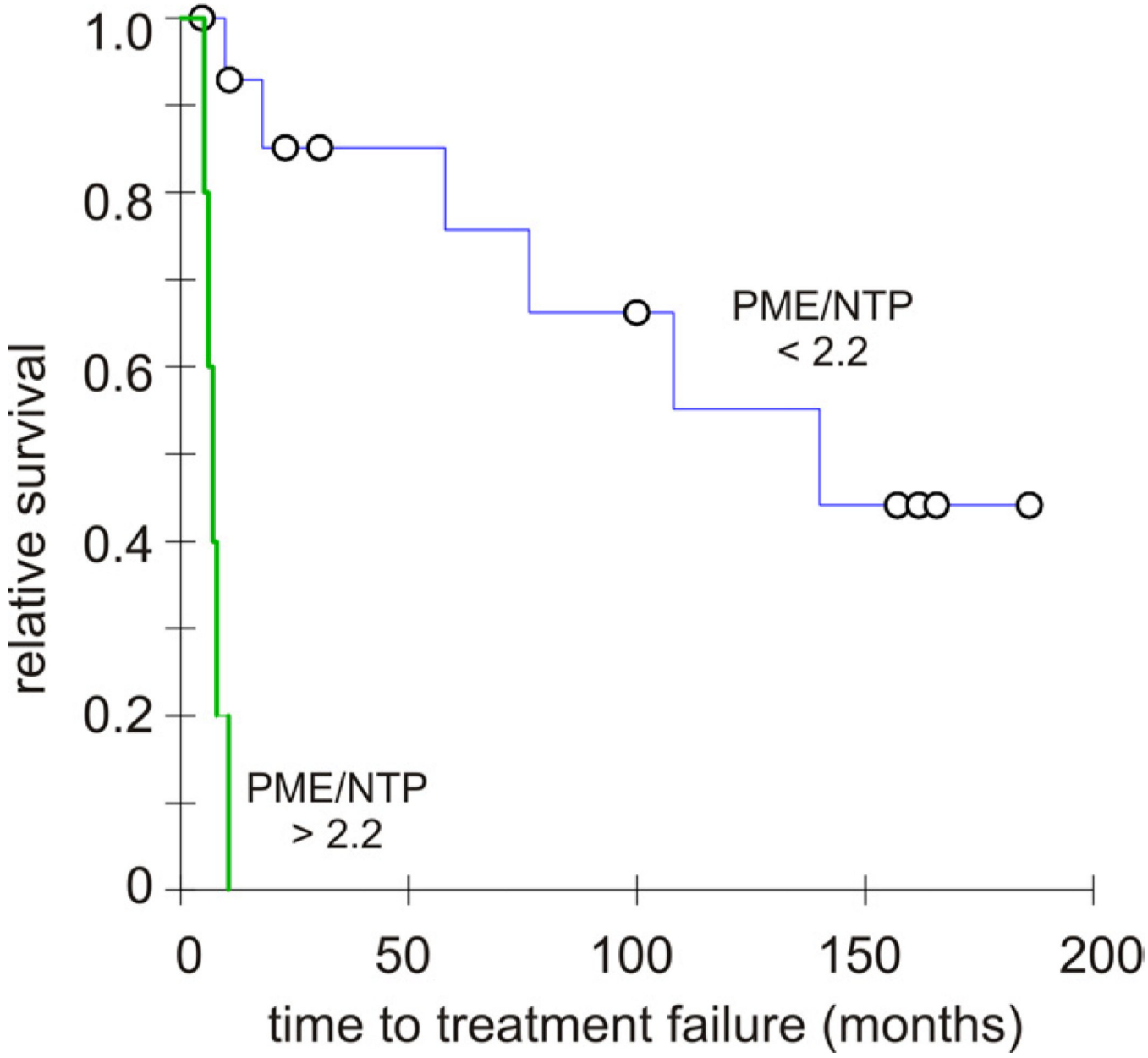

FIGURE 2. Kaplan-Meier curves modeling the Time to Treatment Failure (TTF) of DLBCL patients segregated by the pretreatment PME/NTP tumor value obtained noninvasively by ^{31}P MR spectroscopy

Survival curves of the DLBCL patients set apart by the PME/NTP cutoff that maximized the comparative relative risk to fail treatment (cutoff at 2.2). The blue survival curve belongs to the group below the cutoff while the green survival curve belongs to the group above it with circles corresponding to censor points in both curves. The statistical difference of the survival function curves determined by the Tarone-Ware was highly significant ($p <$ 0.00001) with a comparative relative risk to fail treatment of 8.66.

NIH-PA Author Manuscript
NIH-PA Author Manuscript
NIH-PA Author Manuscript

Acad Radiol. Author manuscript; available in PMC 2014 September 01.

Table 1

Clinical and biological characteristics of the cohort of diffuse large B-cell lymphoma patients

treatment	number	gender	age	stage	IPI[1]	RT6m[2]	TTF[3]	PME/NTP[4]
CHOP[5]:	1	F	68	II	1	CR	+23.0	2.16
	2	F	49	I	2	CR	18.0	0.84
	3	F	48	II	0	CR	+186.0	1.52
	4	M	29	IV	1	PR	9.8	1.85
	5	M	59	III	1	PR	8.0	2.83
	6	F	68	IV	2	CR	+165.7	1.32
	7	M	53	II	1	CR	+157.1	1.92
	8	F	51	III	2	CR	+161.8	1.88
	9	M	77	II	3	PR	+4.7	1.97
	10	F	74	IV	3	CR	140.0	1.32
	11	M	63	III	1	CR	76.4	1.51
	12	M	53	II	1	CR	108.1	1.39
ProMACE-CytaBOM[6]:	13	F	19	III	0	CR	+100.0	1.43
CHOP plus ICE[7]:	14	F	47	IV	4	PR	5.2	2.86
CNOP[8]:	15	M	48	IV	2	CR	58.0	0.86
PMitCEBO[9]:	16	M	85	III	3	PR	7.1	2.59
CHOP-like (not-specified)	17	M	70	III	4	PR	10.5	2.50
	18	F	66	IV	2	PR	6.1	2.65
	19	M	65	I	3	CR	+30.6	1.46
	20	M	58	III	2	CR	+10.8	0.89

[1] IPI: International Prognostic Index

[2] TR6m: treatment response at 6 months (CR: complete response, PR: partial response)

[3] TTF: time to treatment failure (+ denotes censored)

[4] PME/NTP: pretreatment tumor PME/NTP value

[5] CHOP: cyclophosphamide, doxorubicin, vincristine, and prednisone

NIH-PA Author Manuscript

NIH-PA Author Manuscript

NIH-PA Author Manuscript

[6] ProMACE-CytaBOM : CHOP plus etoposide, cytarabine, bleomycin, methotrexate, and leucovorin

[7] ICE : ifosfamide, carboplatin, etoposide

[8] CNOP : cyclophosphamide, mitoxantrone, vincristine, and prednisone

[9] PMitCEBO: CNOP plus etoposide and bleomycin

NIH-PA Author Manuscript
NIH-PA Author Manuscript
NIH-PA Author Manuscript

Table 2

Student t-test analysis of the correlation of response to treatment at six months with the pretreatment tumor PME/NTP and IPI parameters

	complete response[1]			**partial response**[1]			***p*-value**[3]
	mean	**SD**[2]	**n**	**mean**	**SD**	**n**	
PMR	1.42	0.21	13	2.46	0.40	7	0.00001
IPI[4]	2	1	13	3	1	7	0.06

[1] Treatment response at six months. In this cohort there were no cases with stable disease or progressive disease.

[2] Abbreviations: SD, standard deviation; n, number of observations.

[3] The *p*-value refers to the comparison of the mean values of **complete** *vs* **partial response** in each group.

[4] IPI was rounded up to the nearest integer considering the discrete values of IPI

Acad Radiol. Author manuscript; available in PMC 2014 September 01.

NIH-PA Author Manuscript
NIH-PA Author Manuscript
NIH-PA Author Manuscript

Acad Radiol. Author manuscript; available in PMC 2014 September 01.

Table 3

Fisher probability analysis of the correlation of response to treatment at six months with the pretreatment tumor PME/NTP and IPI using the maximum of the Youden index for comparative purposes (left and middle truth tables, respectively) and the pretreatment tumor PME/NTP using the cutoff for maximum sensitivity (right truth table)

		treatment response		
PME/NTP		**CR**[1]	**PR**	total
	≤ 1.92	12	1	13
	> 1.92	1	6	7
	total	13	7	20
		accuracy = 0.90		
		prevalence = 0.65		
		sensitivity = 0.92		
		specificity = 0.86		
		false negative rate = 0.08		
		false positive rate = 0.14		
		positive predictive value = 0.92		
		negative predictive value = 0.86		
		p < 0.001		

		treatment response		
IPI		**CR**	**PR**	total
	≤ 2.0	11	3	14
	> 2.0	2	4	6
	total	13	7	20
		accuracy = 0.75		
		prevalence = 0.65		
		sensitivity = 0.85		
		specificity = 0.57		
		false negative rate = 0.15		
		false positive rate = 0.43		
		positive predictive value = 0.79		
		negative predictive value = 0.86		
		p < 0.07		

		treatment response		
PME/NTP		**CR**	**PR**	total
	≤ 2.2	13	2	15
	> 2.2	0	5	5
	total	13	7	20
		accuracy = 0.90		
		prevalence = 0.65		
		sensitivity = 1.00		
		specificity = 0.71		
		false negative rate = 0.00		
		false positive rate = 0.29		
		positive predictive value = 0.87		
		negative predictive value = 1.00		
		p < 0.001		

[1] Abbreviations: **CR**, complete response; **PR**, partial response